Environmental Science and Pollution Research (2023) 30:52692–52701
https://doi.org/10.1007/s11356-023-26077-3

RESEARCH ARTICLE

Water storage tank used as additional thermal energy for solar air heater

Hakim Semai[1] · **Amor Bouhdjar**[1]

Received: 22 November 2022 / Accepted: 18 February 2023 / Published online: 27 February 2023

Abstract

Research dedicated to renewable energies aims at reducing the negative impact of fossil fuels on the ecosystem and particularly to solar applications so to make it more competitive with conventional systems. In this paper, attention is paid to flat plate solar air collector due to their simplicity and immediate use in converting solar energy, and operating at low temperature. A modification has been brought to one of its components to further improve its performance. To meet the needs of thermal energy demand for a given use (heating, drying, etc.), an installation of a field of collectors (solar air collector, solar water heater, etc.) is required to ensure the demanded thermal power. The modification consists in integrating, on the back of the solar air collector, a water tank supplied by solar water collectors, which serves as a heat storage tank for any other use. A simulation is performed using Fluent CFD code, in order to follow the evolution of the heat transfer fluid flow considering the implantation site meteorological data at Bouzaréah (Algeria). Different flow rates were considered for the two heat transfer fluids. A primary heat transfer fluid was represented by air and the second one represented by water. Simulation results show that thermal efficiency of the modified solar air collector is improved compared to the one of the typical solar air heater when we use forced flow. For the different used flow rates, higher efficiency is obtained when the flow rate of the primary heat transfer fluid (air) is increased.

Keywords Solar air heater · Solar energy · Efficiency · Renewable energy · Solar water heater · Numerical simulation

Introduction

Energy has always been a vital issue for man and human societies. Its availability affects human behavior whether in abundance or in scarcity. Consequently, new challenges will arise particularly for the environment and socio-economic balances. Awareness of the importance of these issues (global warming, depletion of resources, increased costs, etc.) should divert us towards a more rational use of energy, an optimization of implemented energy processes, and more widespread use of renewable energy systems. Among these renewable energies, solar energy has been used for millennia. Techniques for exploiting this resource have considerably improved in recent years involving state-of-the-art technology and making operating costs more attractive, particularly in the production of thermal energy. Thermal energy produced by solar energy is ecological without any greenhouse gas emissions. The present work focuses on solar air flat plate collector.

Solar air collectors suffer from poor thermal efficiency, due to low heat exchange between the absorber and the heat transfer fluid (Alta et al. 2010) as well as heat loss from its various parts (Saxena et al. 2015; Hernandez and Quinonez 2018; Karwa and Srivastava 2013), in particular at glazing (Koyuncu 2006; Youcef and Desmons 2006). One of the proposed solutions consists in generating zones of turbulence in the flow path by the using fins (Khatri et al. 2021; Ho et al. 2012; Mahmood et al. 2015; El-khawajah et al. 2011; Omojaro and Aldabbagh 2010) and roughness (Karwa and Srivastava 2013; Kumar and Prasad 2017). V ribs constitute another way to create roughness and to enhance heat transfer from the surface to the flowing air (Yadav et al. 2021; Kumar et al. 2020, 2021a; Mahanand and Senapati 2021; Patel & Langevar 2019; Thakur et al. 2017; Singh

Responsible Editor: Philippe Garrigues

✉ Hakim Semai
hsemai@yahoo.com; h.semai@cder.dz

[1] Renewable Energy Development Center (CDER), Solar Thermal and Geothermal Energy Division, 16340 Bouzaréah Algiers, Bouzareah, Algeria

et al. 2011, 2012; Sahu and Prasad 2017; Kumar and Layek 2019). The presence of turbulences improves heat exchange and the fins or the ribs increase the heat exchange area. The different studies consider parameters in order to optimize configurations.

In order to increase the low heat transfer, other studies consider forced air solar heater based on air impinging on flat surface of absorber plate. According to authors (Zukowski 2015), the new configuration improves the energy conversion efficiency and reduces the pressure losses.

Other works suggest the use of thermal energy storage system (Tyagi et al. 2021; Saxena et al. 2020; Wadhawan et al. 2018; Fath 1995; Rasheed 2020; Duan et al. 2021), by means of sensible heat storage materials (Kumar et al. 2021b; Alkilani et al. 2011; Gautam and Saini 2020; Saxena and Goel 2013; Pradyumna and Debendra 2017; Saxena et al. 2013; Prasad et al. 2019; Kumar et al. 2016). A particular case was the use of granular carbon on the absorber in order to stabilize the exit temperature (Patel & Langevar 2019). Latent heat storage materials (PCM) was also used in order to reduce losses to the outside environment (Quanquan et al. 2022; El Khadraoui et al. 2016; Ke et al. 2021; Salih et al. 2020). PCM paraffin filling the vacuum tube of heat pipe was investigated with a purpose of improving the efficiency of the heat transfer. In the case, aluminum fins were used to contain the PCM paraffin and to extend the heat transfer area Wang & al. 2021).

In the present work, we are interested in geometry modification of the solar air flat plate collector in which the collector back made of an insulation panel will be replaced by a water-filled tank. The water tank that acts as a storage system in a solar water heater is used as a back-up system for the solar air collector. Generally, a field of solar collectors is used to respond to thermal energy needs expressed by a consumer for a given purpose (heating, drying, etc.). The modified solar flat plate air collector will avoid the realization complexity of storage tank separately, which is generally of a cylindrical shape, free more space, improve the thermal efficiency of the solar air heater (SAH), and generate a stabilized exit temperature.

The objective of this study is to analyze the energy contribution of the storage system to the performance of solar air collectors.

Physical model of the solar air heater

A solar collector benchmark is set up at the Renewable Energy Development Center. The benchmark is made of a solar air heater, a solar water heater, and a mixed solar collector (air-water). The daily follow-up of the recorded data from the benches, during test periods and their analysis showed the following (Bouhdjar et al. 2021):

- A low thermal efficiency of the SAH; even the use of baffles placed in the flow vein to increase the exchange surface does not have a noteworthy effect on thermal efficiency.
- The use of a mixed solar collector (air-water) in order to reduce heat losses to the outside environment has had a positive impact on the instantaneous efficiency compared to the two other collectors combined (water collector and air collector), but it remains below the required threshold.
- The set-up of a storage tank requires professional intervention and additional space.

Replacing the back insulation of the collector with a water tank as a back-up system avoids the aforementioned drawbacks. Moreover, the new configuration will not generate additional costs because the component is an integral part of the solar water heater and even allows a reduction in cost with a simple realization without the intermediary intervention.

The storage tank fed by water coming from the solar water heater will be adjusted to the shape of the air collector back. Thus, the data collected at the level of the solar water heater (outlet water temperature), available at the level of the test bench, will be used as a boundary condition for the solar flat plate air collector. The modified solar air heater (MSAH) considered in the study has a shape similar to the one set up in the test bench. Results from the later will be considered for validation.

Figure 1 shows a scheme of typical SAH and Fig. 2 shows a scheme of the MSAH.

Figure 3 shows the test benches made of solar air heater and solar water heater designed and used for the experiment.

Table 1 shows dimensions of the solar air heater and the modified solar air collector.

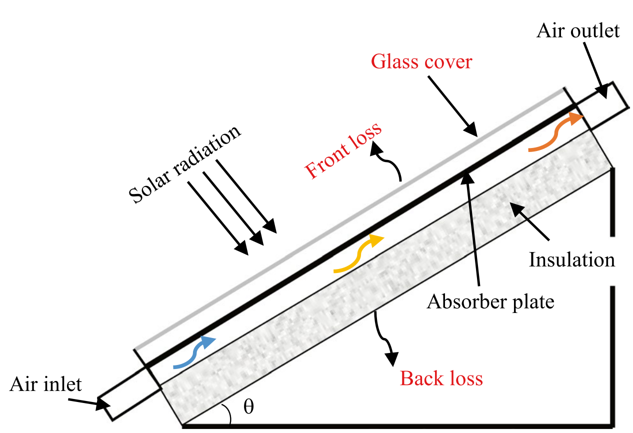

Fig. 1 Typical solar air heater (SAH)

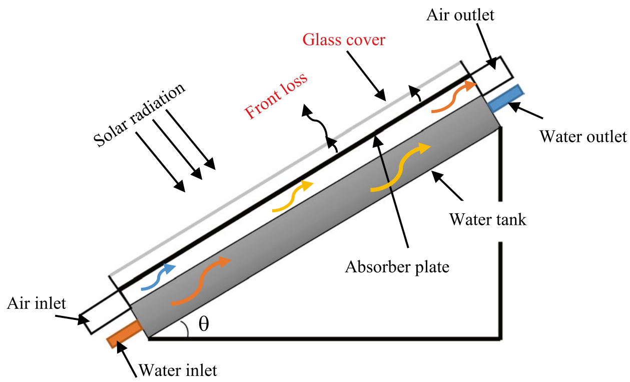

Fig. 2 Modified solar air heater (MSAH)

Mathematical model and boundary conditions

Governing equations

CFD methods consist of numerical solutions of mass, momentum, and energy conservation equations along with other equations such as species transport.

The following equations summarize the governing equations:

Continuity equation

$$\frac{\partial \rho}{\partial t} + \nabla.\left(\rho\vec{v}\right) = 0 \tag{1}$$

Momentum equation

$$\frac{\partial\left(\rho\vec{v}\right)}{\partial t} + \nabla.\left(\rho\vec{v}\,\vec{v}\right) = \rho\vec{g} - \nabla p + \nabla.\left(\overline{\tau}\right) + \vec{F} \tag{2}$$

Energy equation

$$\frac{\partial(\rho E)}{\partial t} + \nabla.\left(\vec{v}\,(\rho E + p)\right) = \nabla.\left(k_{eff}\nabla T + \left(\overline{\tau_{eff}}.\vec{v}\right)\right) \tag{3}$$

where p is the static pressure, $\overline{\tau}$ is the stress tensor, and $\rho\vec{g}$ and $\vec{F}$ are the gravitational body force and external body forces, respectively.

The k-ε model used for turbulent flows is expressed by:

$$\frac{\partial}{\partial t}(\rho k) + \frac{\partial}{\partial x_j}\left(\rho k u_j\right) = \frac{\partial}{\partial x_j}\left(\left(\mu + \frac{\mu_t}{\sigma_K}\right)\frac{\partial k}{\partial x_j}\right) + G_K + G_b - \rho\varepsilon + S_K \tag{4}$$

$$\frac{\partial}{\partial t}(\rho\varepsilon) + \frac{\partial}{\partial x_j}\left(\rho\varepsilon u_j\right) = \frac{\partial}{\partial x_j}\left(\left(\mu + \frac{\mu_t}{\sigma_\varepsilon}\right)\frac{\partial \varepsilon}{\partial x_j}\right) + C_{1\varepsilon}\left(G_K + C_{3\varepsilon}G_b\right) - C_{2\varepsilon}\rho\frac{\varepsilon^2}{K} + S_\varepsilon \tag{5}$$

G_k is the generation of turbulence kinetic energy due to the mean velocity gradients. It is defined by:

$G_k = -\rho\overline{u'_i u'_j}\frac{\partial u_j}{\partial x_i}$;$G_b$ is the generation of turbulence due to buoyancy; σ_k and σ_ε are the turbulent Prandtl numbers for k and ε, respectively, and β is the thermal expansion coefficient which is approximated by $\beta \approx {}^{1}/_{T}$.

Nusselt number

In solar heating system, the convective heat transfer coefficient between the absorber surface and the flowing air is low. Considering the heat transfer from the absorber to a region at the bulk temperature, we can easily express the

Fig. 3 Pictures of solar collector setup: **a** solar flat plate air collector, **b** solar flat plate water collector

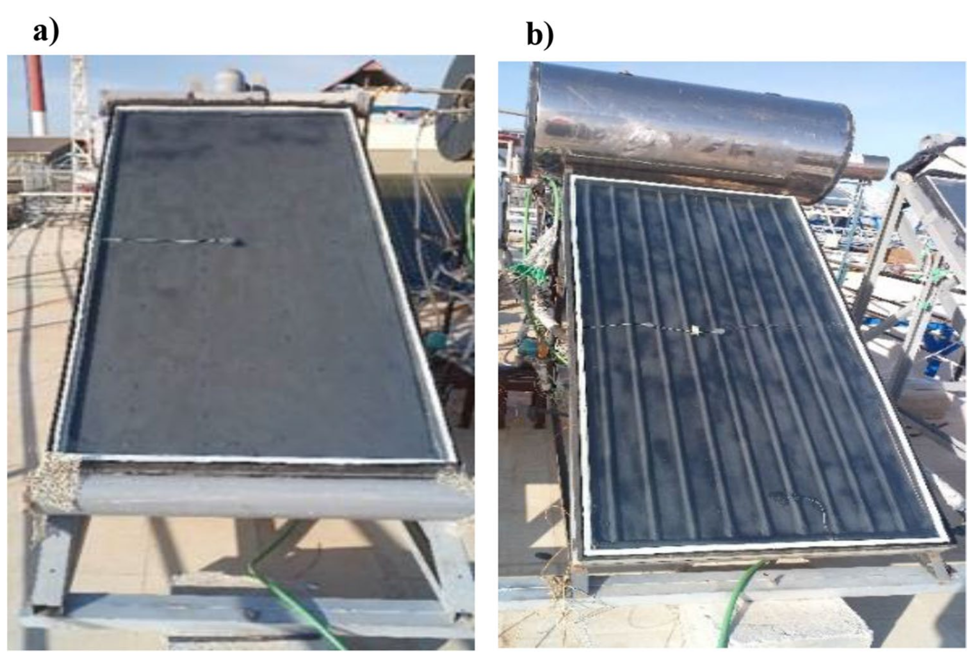

Table 1 Geometrical parameters of solar air heaters (conventional and modified)

Element collector designation	SAH	MSAH
Confined space thickness	0.028 m	0.028 m
Flow vein thickness	0.032 m	0.032 m
Absorber width	0.85 m	0.85 m
Absorber length	1.85 m	1.85 m
Tank volume	–	1.57 m^3
Tank thickness	–	0.1 m
Inlet water duct diameter	–	0.02 m
Tilt angle (θ)	36°	36°

Nusselt number from which we deduce the convection heat transfer coefficient.

The convection heat transfer is expressed by:

$$q_p = h\left(T_{abs} - T_B\right) \tag{6}$$

and from Eq. (6), we deduce the Nusselt number

$$\mathrm{Nu} = \frac{\mathrm{h}D_h}{\lambda} = \frac{\mathrm{q}_P D_h}{\left(\mathrm{T}_{abs} - T_B\right)\lambda} \tag{7}$$

where

q_P
is the heat flux
D_h is the hydraulic diameter
T_{abs} is the absorber mean temperature
T_B is the bulk temperature of fluid and
λ is the thermal conductivity of fluid

Thermal efficiency

The performance of the flat solar collector varies with the geometry of the collector, internal and external parameters such as solar irradiation, ambient temperature, mass flow rate, etc.

The thermal efficiency of the modified solar air heater is defined as follows (Abuska 2018):

$$\eta = \frac{\dot{m}_a C_{pa}\left(T_{fo} - T_{fi}\right)}{IA_c + \dot{m}_w C_{pw}\left(T_{fwo} - T_{fwi}\right)} \tag{8}$$

where

$\dot{m}_a, \dot{m}_w$ is the mass flow rate for air and water, respectively
C_{pa}, C_{pw} is the specific heat for air and water, respectively
T_{fo}, T_{fi} is the outlet and inlet temperatures for air
T_{fwo}, T_{fwi} is the outlet and inlet temperatures for water
I is the solar irradiance and
A_c is the collector area

Boundary conditions

Boundary conditions are defined from the weather conditions at the experimentation site (Bouzaréah, Algeria), solar irradiance as heat source, ambient temperature as inlet air temperature and water inlet temperature (secondary heat transfer fluid), and the latter is the water outlet temperature of the solar water heater. Weather conditions correspond to a clear sky day (Fig. 4).

On the second of January, 2022, solar air heater was operating under natural flow and on the fifth of July, 2021, solar air heater was operating under forced flow. On both days, water from the solar water heater, used as a second heat transfer fluid for the SAH, was operating under forced flow with a mass flow rate of 0.019kg/s.

We observe that solar radiation evolves regularly during the time interval (10–15h30). The maximum radiation recorded is 950W/m^2 and the minimum is a little higher than 600W/m^2, for the natural flow. On the other hand, radiation during the day in which the flow considered is forced varies from 600 to 900 W/m^2. The same observation applies to the air inlet temperature (Tfi), which is generally stable

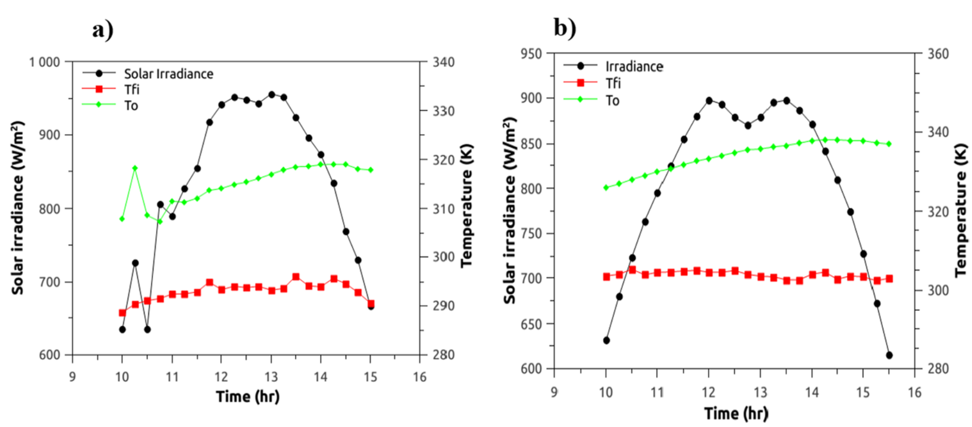

Fig. 4 Solar irradiance, ambient temperature, and water inlet temperature; **a** on the day of 02/01/2022 (natural flow), **b** on the day of 05/07/2021 (forced flow)

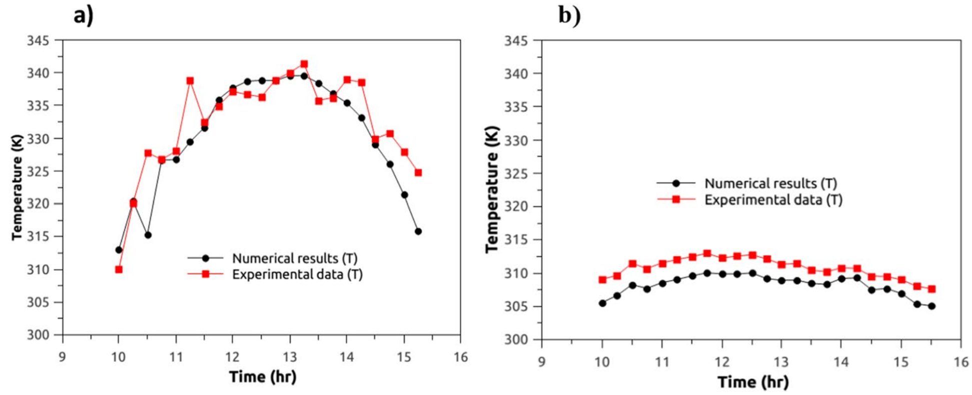

Fig. 5 Experimental data and simulation result for outlet temperatures, **a** for natural flow (on 02/01/2022), **b** for forced flow (on 05/07/2021)

throughout the time interval and evolves at 295 K average for the natural flow and just over 300K for the forced flow. However, the water outlet temperature (To) evolves in an upward and regular manner throughout the test interval with recorded values ranging between 307.9K for the minimum and 319.9K for the maximum, in the case of the natural flow and they are between 325K and 336.9K for the forced flow.

During the day of 02/01/2022, boundaries conditions are as follows:

The collector inlet pressure and the inlet temperature are those of the ambient environment:

$$P_{ri} = 0, T_{inlet} = T_{\infty} \tag{9}$$

Pressure outlet is the duct exit

$$P_{ro} = 0 \tag{10}$$

Sidewalls and bottom wall are adiabatic

$$u = 0, v = 0, \frac{\partial T}{\partial y} = 0 \tag{11}$$

Incident solar irradiance on the transparent cover is given in Fig. 4.

$$u = 0, v = 0, q = I \tag{12}$$

The physical properties of the air are assumed constant at bulk temperature.

During the day of 05/07/2021, the boundary conditions are:

The air mass flow is measured at the collector inlet, and the temperature is the ambient temperature:

$$\dot{m}_a = 0.075 \left({}^{kg}/{}_{s} \right), T_{inlet} = T_{\infty} \tag{13}$$

The water mass flow rate is identical for all tests.

Outflow conditions are considered at the duct exit

$$\frac{\partial u}{\partial x} = 0, \quad \frac{\partial v}{\partial x} = 0, \quad \frac{\partial T}{\partial x} = 0 \tag{14}$$

Sidewalls and bottom wall are adiabatic

$$u = 0, v = 0, \frac{\partial T}{\partial y} = 0 \tag{15}$$

Validation of the numerical simulation

The validation of the code requires its implementation on an existing experimental model of the benchmark according to the operating conditions, namely solar radiation and ambient temperature.

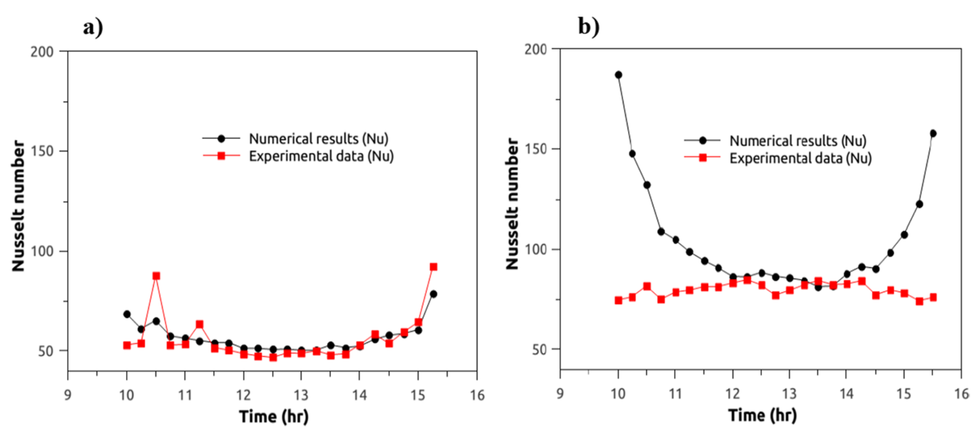

Fig. 6 Experimental data and simulation results for Nusselt number, **a** for natural flow (on 02/01/2022), **b** for forced flow (on 05/07/2021)

Figures 5, 6, and 7 show SAH outlet temperatures, Nusselt number, and instantaneous efficiency, respectively. Outlet air temperatures obtained from simulation and from experiment follow the same trend during the entire time interval in both flow regimes (Fig. 5). A 0.9% average deviation for the forced flow case and 0.95% average deviation for the natural one are observed. The average deviation for Nusselt numbers is 8.58% for natural flow and 15% for the forced flow (Fig. 6). Figure 7 shows system performances calculated by simulation model and the ones obtained from experiment data analysis. The curves have the same trend and average differences of about 13% for forced flow and 8.4% for the natural flow are observed.

Nevertheless, comparing the results for the two flow regimes (natural and forced), it can be seen that temperatures recorded with a natural flow far exceed the ones obtained with a forced flow. In natural flow regime, the crossing time being much longer allows a lasting contact between the fluid and the absorber plate. This leads to a further temperature increase. However, the efficiency is much higher for a forced flow since it is proportional to the amount of energy transported by the heat transfer fluid. Forced flow means a high flow rate and therefore a larger airflow mass and therefore a greater amount of energy transported. The same situation is noticed for the Nusselt number, which characterizes the enhancement of heat transfer through a fluid as result of convection.

Due to the successful comparison between the experimental data and numerical simulation results, the code is considered valid.

Results and interpretation

Using the previously validated Fluent CFD code, a numerical simulation was performed on a typical SAH and on the modified SAH previously described in which a storage water tank replaces the collector back insulation. The storage tank is fed from a solar water heater. The water tank acts also as insulator for the air collector. As mentioned previously, the SAH is operating under natural fluid flow in one case and in forced fluid flow at a rate of 0.075kg/s in another case. As for the water coming from the solar water heater to the storage tank on the back of the SAH, the mass flow rate is equal to 0.019kg/s.

Figure 8 shows outlet air temperatures for both configurations of solar air heaters (MSAH, SAH). An improvement of the outlet temperature is obtained with the MSAH. Temperature increase is around 3K for forced flow. However, with natural flow, the temperature is lower in the same MSAH compared to the SAH. In natural flow, higher temperature is obtained with the modified air collector compared to the same collector in a forced flow regime. More energy is transferred from water to the air. Also for the Nusselt number, there is no improvement with the modified model (Fig. 9), for the case of a natural air flow.

The instantaneous efficiency of the SAH in forced flow hardly exceeds 30%. However, with the MSAH, a substantial improvement is obtained with the efficiency exceeding 45%, and this represents a 57% increase compared to the typical SAH (Fig. 10). It can be observed on the efficient curve that the performance of the SAH follows the same trend as solar radiation, the only used heat source. However, for the MSAH, the efficiency does not follow the same path as solar irradiance. Due to the energy supplied by storage tank, it continues increasing even after sunset.

The temperature rise with the forced flow regime results from the use of hot water coming from the solar water collector, which comes as additional energy supplier to the solar air collector. This increase coupled with a forced flow improves the performance of the MSAH, as confirmed by the performance curve given in Fig. 10.

The new configuration makes the system operate over a longer time with a stabilized exit temperature.

As far as the comparison of the flow régime, the efficiency is better with the one of forced flow, as given by

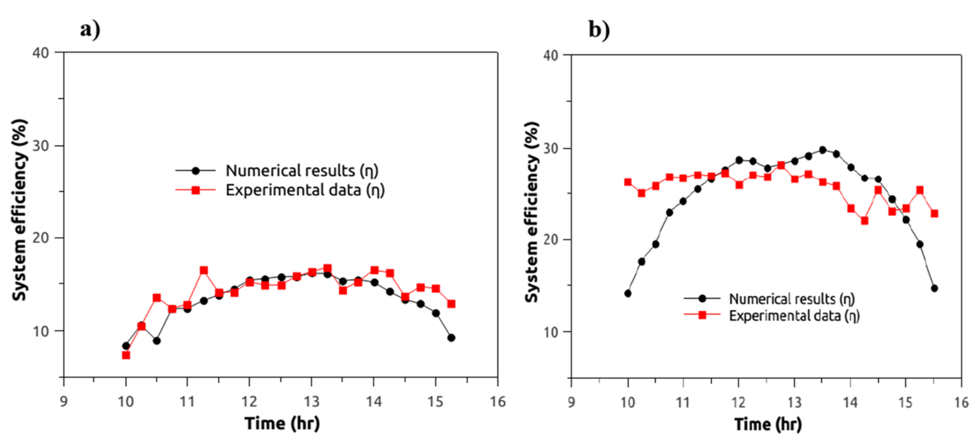

Fig. 7 Experimental data and simulation result for the instantaneous efficiency, **a** for natural flow (on 02/01/2022), **b** for forced flow (on 05/07/2021)

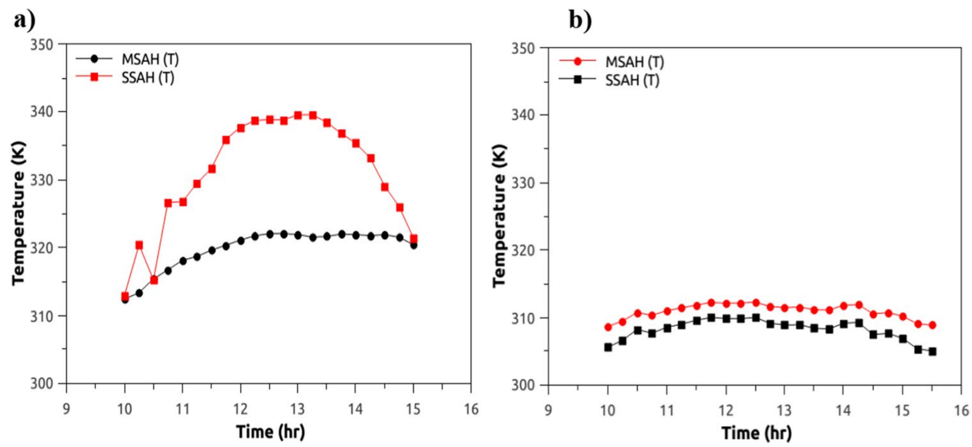

Fig. 8 Outlet temperatures in both configurations (SAH and MSAH), **a** for natural flow (on 02/01/2022), **b** forced flow (on 05/07/2021)

the validation curves. This due to a minimizing losses to the outside environment but with a slight improvement because of the absorber cooling, if the flow rate increases, and consequently decreasing a heat exchange rate between the absorber and the heat transfer fluid. With the MSAH, the flow rate can be increased further with no risk at lowering further the absorber temperature due to a significant heat exchange from the heat transfer fluid of the water collector. The latter will continuously be renewed by hot water coming from the solar water collectors. The consequence of this system is to stabilize the exit air temperature for any purpose whether it be for drying or building heating.

We studied also the effect of different flow rates for air and water in order to analyze which of the heat transfer fluids will have the most impact on the collector performance. Initially, the air flow rate is fixed at 0.075 kg/s and the water flow rate takes different values (0.013, 0.019, and 0.027 kg/s). In another simulation, the water flow rate is fixed at 0.019 kg/s and the air flow rate takes different values (0.005, 0.019 and 0.075 kg/s).

Figure 11 shows the outlet temperatures for MSAH model for different flow rates. The impact of the air flow rate (primary heat transfer fluid) far outweighs the water flow rate (secondary heat transfer fluid). The temperature difference between the two heat transfer fluids (air and water) can reach 21K. Increasing the flow rate of the secondary fluid (water) will have slight influence on the outlet temperature of the heat transfer fluid (air) because the quantity of energy transported by the latter will be smaller compared to the one of high airflow. The energy evacuated would be more important when increasing the flow rate as confirmed by the efficiency curve as long as it is partly proportional to the flow rates (Fig. 12).

Similar result is obtained for the Nusselt number. The increase in the flow rate of the secondary fluid does not improve the temperature gradient at the absorber surface as long as the main heat transfer fluid (air) is fixed at 0.019kg/s. However, if the flow rate of the primary heat transfer fluid (air) is increased while fixing that the one of secondary fluid (water), Nusselt number is improved. Increasing the main fluid flow (air) beyond a threshold does not improve Nusselt number. With the highest flow rate for the main fluid flow (0.075 kg/s), Nusselt number is lower than the one obtained with a lower flow rate (0.019kg/s) (Fig. 13).

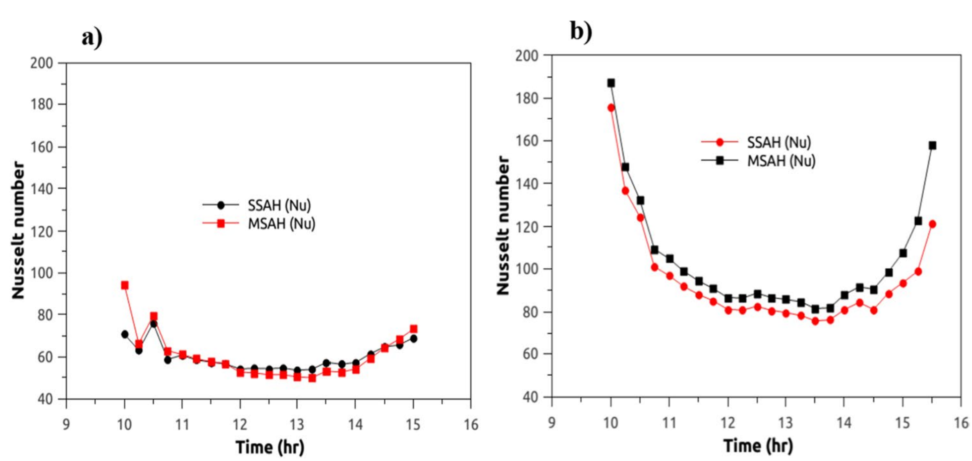

Fig. 9 Nusselt number for both configurations (SSAH and MSAH), **a** for natural flow (on 02/01/2022), **b** forced flow (on 05/07/2021)

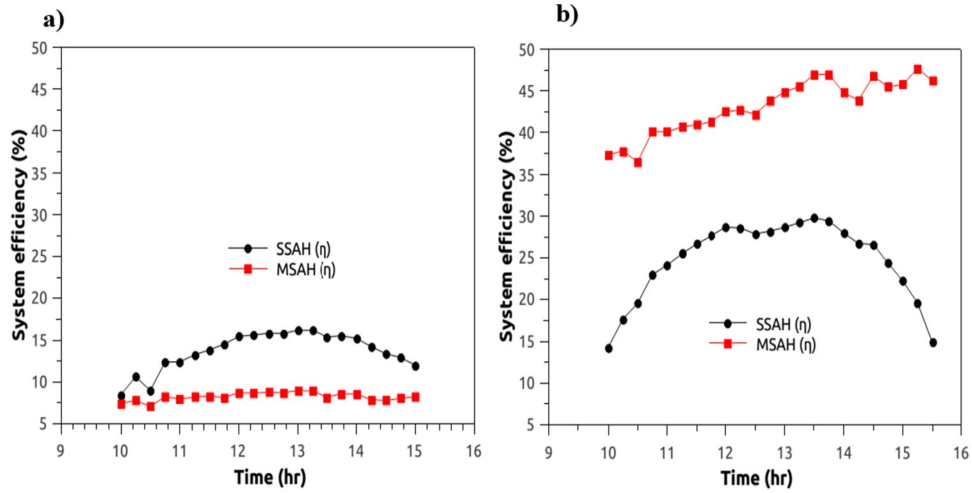

Fig. 10 Instantaneous efficiency for both configurations (SAH and MSAH), **a** for natural flow (on 02/01/2022), **b** forced flow (on 05/07/2021)

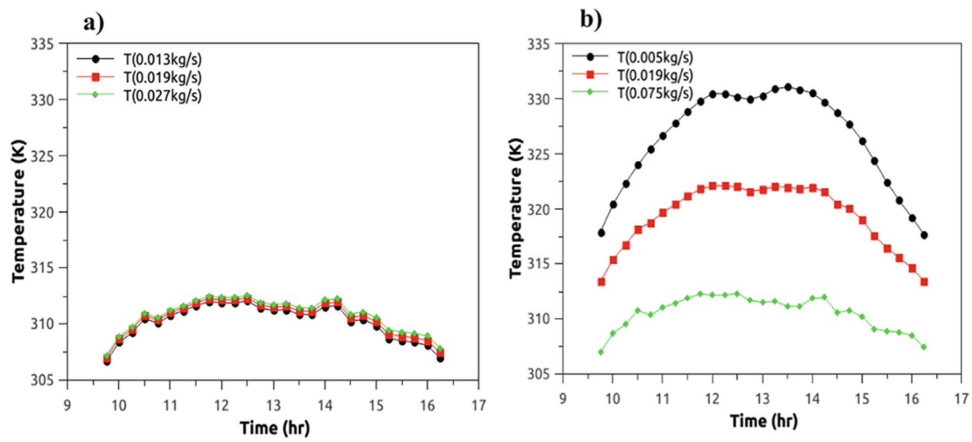

Fig. 11 Outlet temperature, **a** variable water flow, **b** variable airflow

Conclusion

Typical solar air collector is considered. Some modifications are made on the initial solar air heater configuration replacing the back insulation with water storage tank. In order to assess the thermal efficiency of the two configurations, a numerical study using fluent CFD code was applied. The developed numerical model has been validated through experimental results. Different flow rates were considered for the two heat transfer fluids which are air as a primary heat transfer fluid and water as the second heat transfer fluid. From simulation results, we conclude that:

- Forced flow gives better performance rather than natural flow.

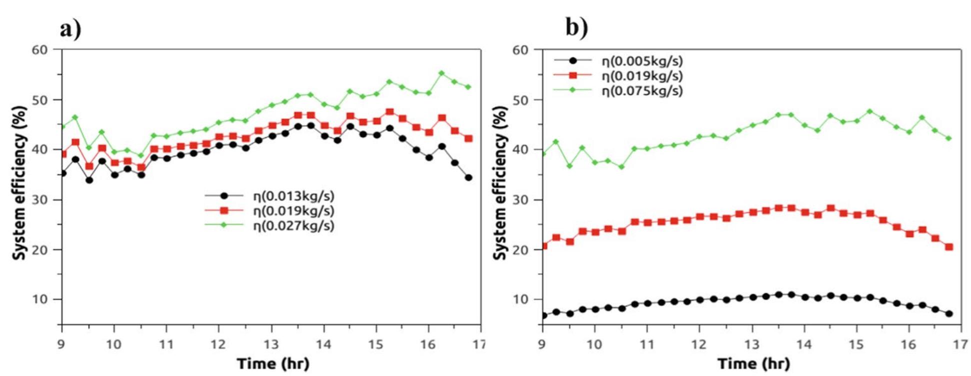

Fig. 12 Instantaneous efficiency, **a** variable water flow, **b** variable airflow

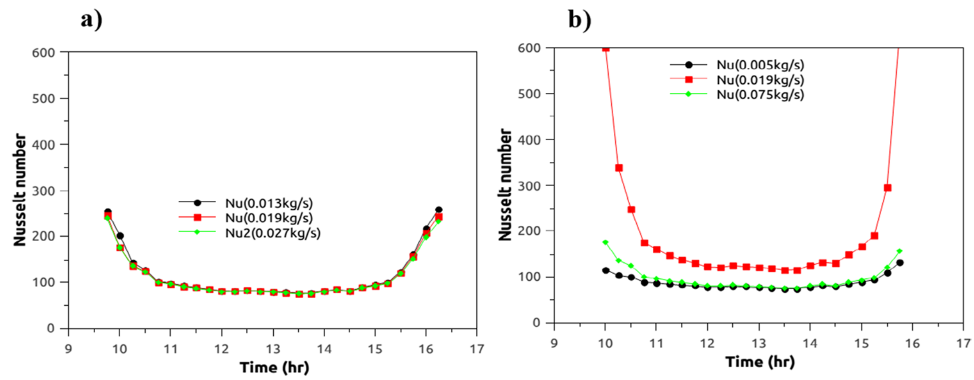

Fig. 13 Nusselt number, **a** variable water flow, **b** variable airflow

- Thermal efficiency of the modified model is better than that of the typical one for forced flow regime.
- For the considered flow rates, best efficiency is obtained when the air flow rate is increased.
- The increase of the water flow rate has a slight influence on the solar air heater efficiency.

Results show that modification made on a typical solar flat plate air collector has a considerable impact on the solar air heater thermal performance. Modified solar air collector might deliver heat or temperature according to the need whether in drying or building heating through a regulation system. Moreover, its construction will not require additional cost since the storage tank is an equipment, which is part of a solar system, and is moved to the solar air collector. Performance, flexibility and cost make the new solar air collector model more attractive for the development of solar energy system.

Author contributions All authors contributed to the study conception and design. Hakim Semai and Amor Bouhdjar performed material preparation, data collection, and analysis. Hakim Semai wrote the first draft of the manuscript and all authors commented on previous versions of the manuscript. All authors read and approved the final manuscript.

Data availability Not applicable for this section.

Declarations

Ethical approval All authors agreed with the content and that all gave explicit consent to submit and that they obtained consent from the responsible authorities at the institute/organization where the work has been carried out, before the work is submitted.

Consent to participate All authors agreed with the content and that all gave explicit consent to submit and that they obtained consent from the responsible authorities at the institute/organization where the work has been carried out, before the work is submitted.

Consent to publish All authors agreed with the content and that all gave explicit consent to submit and that they obtained consent from the responsible authorities at the institute/organization where the work has been carried out, before the work is submitted.

Competing interests The authors declare no competing interests.

References

Abuska M (2018) Energy and exergy analysis of solar air heater having new design absorber plate with conical surface. Appl Therm Eng 131:115–124. https://doi.org/10.1016/j.applthermaleng.2017.11.129

Alkilani MM, Sopian K, Alghoul MA, Sohif M, Ruslan MH (2011) Review of solar air collectors with thermal storage units. Renew Sustain Energy Rev 15:1476–1490. https://doi.org/10.1016/j.rser.2010.10.019

Alta D, Emin Bilgili M, Ertekin C, Yaldiz O (2010) Experimental investigation of three different solar air heaters Energy and exergy analyses. Appl Energy 87:2953–2973

Bouhdjar A, Semai H, Amari A (2021) New technique to evaluate the overall heat loss coefficient for a flat plate solar collector. J Energy Technol Res 14:11–25

Duan J, Liu Y, Zeng L, Wang Y, Su Q, Wang J (2021) Experimental investigation of a novel solar energy storage-heating radiator with phase change material. ACS Omega 6:13601–13610. https://doi.org/10.1021/acsomega.1c00138

El Khadraoui A, Bouadila S, Kooli S, Guizani A, Farhat A (2016) Solar air heater with phase change material: an energy analysis and a comparative study. Appl Therm Eng 107:1057–1064

El-khawajah MF, Aldabbagh LBY, Egelioglu F (2011) The effect of using transverse fins on a double pass flow solar air heater using wire mesh as an absorber. Sol Energy 85(7):1479–1487

Fath HES (1995) Transient analysis of thermosiphon solar air heater with built-in latent heat thermal energy storage system. Renew. Energy 6:119–124. https://doi.org/10.1016/0960-1481(94)00050-G

Gautam A, Saini RP (2020) A review on sensible heat based packed bed solar thermal energy storage system for low temperature applications. Sol Energy 207:937–956. https://doi.org/10.1016/j.solener.2020.07.027

Hernandez AL, Quinonez JE (2018) Experimental validation of an analytical model for performance estimation of natural convection solar air heating collectors. Renew Energy 117:202–216

Ho CD, Chang H, Wang RC, Lin CS (2012) Performance improvement of a double-pass solar air heater with fins and baffles under recycling operation. Appl Energy 100(C):155–163

Karwa R, Srivastava V (2013) Thermal performance of solar air heater having absorber plate with V-down discrete rib roughness for space-heating applications. J Renew Energy 2013:151578. https://doi.org/10.1155/2013/151578

Ke W, Ji J, Xu L, Yu B, Tian X, Wang J (2021) Numerical study and experimental validation of a multi-functional dual-air-channel solar wall system with PCM. Energy 227:120434

Khatri R, Goswami S, Anas M et al (2021) Design and material selection for sustainable development of a novel double pass solar air

heater with porous fins. Proceedings, Materials Today. https://doi.org/10.1016/j.matpr.2021.12.275
Koyuncu T (2006) Performance of various designs of solar air heaters for crop drying applications. Renewable Energy 31(7):1073–1088
Kumar A, Layek A (2019) Nusselt number and friction factor correlation of solar air heater having twisted-rib roughness on absorber plate. Renew Energy 130:687–699. https://doi.org/10.1016/j.renene.2018.06.076
Kumar D, Prasad L (2017) Heat transfer augmentation of various roughness geometry used in solar air heaters. Int J Mech Eng Technol. 8(12):491–508
Kumar PG, Balaji K, Sakthivadivel D, Vigneswaran VS, Velraj R, Kim SC (2021a) Enhancement of heat transfer in a combined solar air heating and water heater system. Energy 221:119805
Kumar R, Nadda R, Kumar S et al (2021b) Heat transfer and friction factor correlations for an impinging air jets solar thermal collector with arc ribs on an absorber plate. Sustainable Energy Technol Assess 47:101523. https://doi.org/10.1016/j.seta.2021.101523
Kumar R, Nadda R, Rana A, Chauhan R, Chandel SS (2020) Performance investigation of a solar thermal collector provided with air jets impingement on multi V-shaped protrusion ribs absorber plate. Heat Mass Transf 56(3):913–930
Kumar S, Prasad RK, Singh KDP (2016) A review on packed bed solar air heating system. Int J Latest Res Eng Technol 2(6):9–16
Mahanand Y, Senapati JR (2021) Thermo-hydraulic performance analysis of a solar air heater (SAH) with quarter-circular ribs on the absorber plate: a comparative study. Int J Therm Sci 161:106747
Mahmood AJ, Aldabbagh LBY, Egelioglu F (2015) Investigation of single and double pass solar air heater with transverse fins and a package wire mesh layer. Energy Convers Manage 89:599–607
Omojaro AP, Aldabbagh LB (2010) Experimental performance of single and double pass solar air heater with fins and steel wire mesh as absorber. Appl Energy 87(12):3759–3765
Pradyumna KC, Debendra CB (2017) Solar air heater for residential space heating. Energy Ecol Environ 2(6):387–403
Prasad DMR, Senthilkumar R, Lakshmanarao G (2019) A critical review on thermal energy storage materials and systems for solar applications. Energy 7:507–526. https://doi.org/10.3934/energy.2019.4.507
Quanquan L, Baoguo L, Zhen W, Shuqiang S, Honghai X (2022) A study of unidirectional spiral tube for air evacuation in a solar heater with phase-change material. J Build Eng 46:103659. https://doi.org/10.1016/j.jobe.2021.103659
Rasheed MH (2020) Performance enhancement of solar air heater using different phase change materials (PCMs). J Adv Res Fluid Mech Therm Sci 66:64–75
Sahu MK, Prasad RK (2017) Thermohydraulic performance analysis of an arc shape wire roughened solar air heater. Renew Energy 108:598–614. https://doi.org/10.1016/j.renene.2017.02.075
Salih SM, Jalil LM, Najim SE (2020) Comparative study of novel solar air heater with and without latent energy storage. J Energy Storage 32:101751. https://doi.org/10.1016/j.est.2020.101751
Saxena A, Agarwal N, Cuce E (2020) Thermal performance evaluation of a solar air heater integrated with helical tubes carrying phase change material. J. Energy Storage 30:101406. https://doi.org/10.1016/j.est.2020.101406
Saxena A, Goel V (2013) Solar air heaters with thermal heat storages. Chinese J Eng 2013:1–11. https://doi.org/10.1155/2013/190279
Saxena A, Varun E-SAA (2015) A thermodynamic review of solar air heaters. Renew & Sustain Energy Rev 43(c):863–890
Saxena A, Agarwal N, Srivastava G (2013) Design and performance of a solar air heater with long term heat storage. Int J Heat Mass Transf 60:8–16. https://doi.org/10.1016/j.ijheatmasstransfer.2012.12.044
Singh S, Chander S, Saini JS (2012) Exergy based analysis of solar air heater having discrete V-down rib roughness on absorber plate. Energy 37(1):749–758. https://doi.org/10.1016/j.energy.2011.09.040
Sing Patel S, Lanjewar A (2019) Experimental and numerical investigation of solar air heater with novel V-rib geometry. J Energy Storage 21:750–764. https://doi.org/10.1016/j.est.2019.01.016
Singh S, Chander S, Saini JS (2011) Thermal and effective efficiency based analysis of discrete V-down rib-roughened solar air heaters. J Renew Sustain Energy 3:023107. https://doi.org/10.1063/1.3574430
Thakur DS, Khan MK, Pathak M (2017) Performance evaluation of solar air heater with novel hyperbolic rib geometry. Renew Energy 105:786–797. https://doi.org/10.1016/j.renene.2016.12.092
Tyagi VV, Nagilla DK, Selvaraj J, Chopra K, Kothari R, Pandey AK (2021) Thermal energy storage in phase change material integrated solar collectors for air heating application. IOP Conf Ser Mater Sci Eng 1127:012006. https://doi.org/10.1088/1757-899x/1127/1/012006
Wadhawan A, Dhoble AS, Gawande VB (2018) Analysis of the effects of use of thermal energy storage device (TESD) in solar air heater. Alex Eng J 57:1173–1183. https://doi.org/10.1016/j.aej.2017.03.016
Wang T, Zhao Y, Diao Y, Ma C, YubinZhang XL (2021) Experimental investigation of a novel thermal storage solar air heater (TSSAH) based on flat micro-heat pipe arrays. Renew Energy 173:639–651. https://doi.org/10.1016/j.renene.2021.04.027
Yadav AS, Dwivedi MK, Sharma A et al (2021) CFD based heat transfer correlation for ribbed solar air heater. Proceedings, Materials Today. https://doi.org/10.1016/j.matpr.2021.12.382
Youcef-Ali S, Desmons JY (2006) Numerical and Experimental Study of a Solar Equipped with Offset Rectangular Plate Fin Absorber Plate. Renew Energy 31(13):2063–2075
Zukowski M (2015) Experimental investigations of thermal and flow characteristics of a novel microjet air solar heater. Appl Energy 142:10–12. https://doi.org/10.1016/j.apenergy.2014.12.052